Substrate coupling effect to transport in nanographene ribbon

2009 J. Phys.: Condens. Matter 21 235302

(http://iopscience.iop.org/0953-8984/21/23/235302)

J. Phys.: Condens. Matter **21** (2009) 235302 (5pp) doi:10.1088/0953-8984/21/23/235302

Substrate coupling effect to transport in nanographene ribbon

Shih-Jye Sun

Department of Applied Physics, National University of Kaohsiung, Kaohsiung 811, Taiwan, Republic of China

E-mail: sjs@nuk.edu.tw

Received 23 February 2009, in final form 7 April 2009
Published 13 May 2009
Online at stacks.iop.org/JPhysCM/21/235302

Abstract
Due to the components of electronics being developed on substrates, the substrate coupling to the conduction channel of electronics should be reasonably considered. We propose a nanographene ribbon coupling with substrates to study the variation in conductivity and magnetoresistance.

1. Introduction

Based on the requirement for miniaturization in electronics, nanoelectronics are getting more important. Carbon-compound-based materials, such as carbon nanotubes (CNT), have attracted a great deal of attention due to their electronic or industrial applications [1–3] in the future. A CNT can be made by rolling a two-dimensional graphite layer into a cylindrical tube with various axis directions [4]. The simplest structure of graphite layer is graphene [5], a one-atom-thick material which has been confirmed to be produced in recent experimental reports [6, 7]. Graphene has extremely high conductivity with giant intrinsic carrier mobilities [8]. In addition, experimental results also indicate that graphene's conductivity never falls below a minimum value corresponding to the quantum unit of conductance [9], and that the carriers can transport ballistically in graphene over submicron distances [5]. In terms of valence bonding, the electrical conduction of graphene is established by means of the neighboring π orbits overlapping, and these π orbits are perpendicular to the graphene plane [10]. Many recent proposals attest to the graphene ribbon's potential for nanoelectronics [11–13]. However, it has been proven that a perfect two-dimensional (2D) crystal cannot exist in free space at finite temperature [14]. Fortunately, this 2D instability can be reduced in quasi-2D systems, for instance, growing a 2D material on a perfect surface of bulk material with coupling.

In this study we propose a nanographene ribbon (NGR) which lies on an insulating substrate with a matching crystal lattice, having two metallic electrode connections on both sides. Because the π orbits of the NGR can couple with the orbits of the substrate, the coupling will influence the conduction of the NGR performed by the π orbits, subject to the fact that different substrates produce different coupling to the NGR. Some efforts in utilizing the substrate coupling to tailor graphene for applications have been made [15, 16]. In this paper, for all calculations, the temperature is set at room temperature, $T = 300$ K.

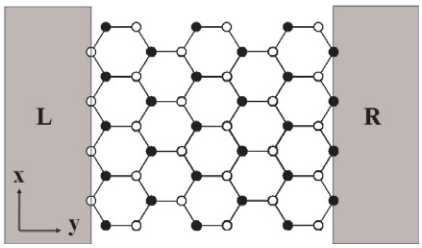

Figure 1. Top view of our hypothetical sample, a zigzag-head NGR, composed of honeycomb unit cells (two sublattices represented by black and white sites), with finite width in the y direction and infinitely long and periodic in the x direction, lies on a substrate (not shown in this figure) and contacts metallic electrodes (gray color) by both zigzag heads.

This paper is organized as follows. In section 2, we describe the model and present the derivation of the theory. In section 3, we present the results of theoretical calculations with their discussion, and draw a brief conclusion.

2. Description of theory

A zigzag-head NGR, with finite width in the y direction and infinitely long and periodic in the x direction, lies on a substrate and contacts metallic electrodes by both zigzag heads: the top view of a hypothetical sample is depicted in figure 1. For the periodicity in the x direction, this NGR can

be considered to be one-dimensional with N point sites along the width direction. The N point sites follow the relation, $N = 2n_{\square} + 2$, where $n_{\square}$ is the number of honeycomb unit cells in the width, for instance, $n_{\square} = 5$ and $N = 12$ in figure 1. Based on the NGR's coupling with the substrate, we propose a hybridization model to simulate the coupling interaction. After the Fourier transformation for periodic x direction, the Hamiltonian description is

$$\begin{aligned} H = & \sum_{k,\alpha\in \mathrm{L,R}} \epsilon_{k,\alpha} c^{\dagger}_{k,\alpha} c_{k,\alpha} + e_p \sum_{k_x} \sum_{i=1}^{N} d^{\dagger}_i(k_x) d_i(k_x) \\ & \times \sum_{k_x} \sum_{i=1}^{N} t_i(k_x)(d^{\dagger}_i(k_x) d_{i+1}(k_x) + \mathrm{h.c.}) \\ & + e_m \sum_{k_x} \sum_{i=1}^{N} a^{\dagger}_i(k_x) a_i(k_x) \\ & + V \sum_{k_x} \sum_{i}^{N} (a^{\dagger}_i(k_x) d_i(k_x) + \mathrm{h.c.}) \\ & + V_{\mathrm{L}} \sum_{k_x} \sum_{k,\mathrm{L}} (c^{\dagger}_{k\mathrm{L}}(k_x) d_{\mathrm{L}}(k_x) + \mathrm{h.c.}) \\ & + V_{\mathrm{R}} \sum_{k_x} \sum_{k,\mathrm{R}} (c^{\dagger}_{k\mathrm{R}}(k_x) d_{\mathrm{R}}(k_x) + \mathrm{h.c.}), \end{aligned} \tag{1}$$

where c and d represent second quantization operators for carriers in the metallic electrodes and NGR, respectively; the a operator represents the carrier in the substrate that couples with the NGR orbits. The first term of the Hamiltonian represents the kinetic energy of carriers in the left and right metallic electrodes. The second term represents the specific orbital energy level of the NGR, e_p. In the tight-binding model, the third term represents the hopping process in the NGR via the hopping energy $t_i(k_x)$, and $t_i(k_x) = t\cos(k_x a/2)$, as $i = 1, 3, \ldots$ and $t_i(k_x) = t$, as $i = 2, 4, \ldots$, where a is the lattice constant and k_x lies within the Brillouin zone, $-\pi/a \leqslant k_x \leqslant \pi/a$; the fourth term represents the orbital energy level of the substrate, e_m; the fifth term represents the orbits hybridizing between the NGR and substrate via V, and the last two terms represent left and right metallic electrode couplings with the NGR via V_{L} and V_{R} interactions, respectively. In our model, two energies e_m and V are utilized to simulate the substrate which couples with the NGR. The current formula, derived from the Keldysh non-equilibrium Green's function method [17] with bias V_a, is

$$\begin{aligned} I = & \frac{2e}{\hbar} \int \frac{\mathrm{d}\epsilon}{2\pi} \sum_{k_x} [f_{\mathrm{L}}(\epsilon + V_a) - f_{\mathrm{R}}(\epsilon)] T_r \\ & \times \left\{ \frac{\Gamma_{\mathrm{L}}(\epsilon)\Gamma_{\mathrm{R}}(\epsilon)}{\Gamma_{\mathrm{L}}(\epsilon) + \Gamma_{\mathrm{R}}(\epsilon)} \right\} [I_m G^{\mathrm{r}}(k_x, \epsilon)], \end{aligned} \tag{2}$$

where $\Gamma_{\mathrm{L(R)}}$ is the spectral function in the left (right) lead, $f_{\mathrm{L(R)}}$ is the Fermi–Dirac distribution function in the left (right) lead and G^{r} is the retarded Green's function. The hybridization interaction drives the charge exchange between the orbits of the NGR and the substrate, which makes the two original independent orbits, represented by the d and a operators in the Hamiltonian, hybridize into two new orbits, represented by the α and β operators. To transfer the Hamiltonian to new operator bases by $a(k_x) = \cos\theta\alpha(k_x) - \sin\theta\beta(k_x)$ and $d(k_x) = \sin\theta\alpha(k_x) + \cos\theta\beta(k_x)$, we choose a specific θ, followed by $\tan 2\theta = 2V/(e_m - e_p)$, leading to

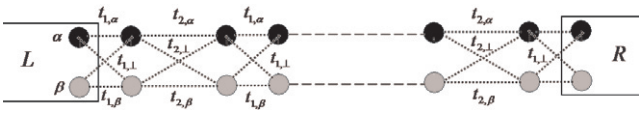

Figure 2. The two-channel model is employed to simulate the substrate-coupled nanographene ribbon, where the left and right end sides are metallic electrodes. The connected lines within the figures represent the carrier hopping paths and are marked by their hopping integrals.

$$\begin{aligned} H = & \sum_{k,\mu\in \mathrm{L,R}} \epsilon_{k,\mu} c^{\dagger}_{k,\mu} c_{k,\mu} + E_{\alpha} \sum_{i,k_x} \alpha^{\dagger}_i(k_x)\alpha_i(k_x) \\ & + E_{\beta} \sum_{i,k_x} \beta^{\dagger}_i(k_x)\beta_i(k_x) + \Bigg(\sum_{i,k_x} t_{i,\alpha} \alpha^{\dagger}_i(k_x)\alpha_{i+1}(k_x) \\ & + \sum_{i,k_x} t_{i,\beta} \beta^{\dagger}_i(k_x)\beta_{i+1}(k_x) \Bigg) + \mathrm{h.c.} \\ & + \Bigg(\sum_{i,k_x} t_{i,\perp} \alpha^{\dagger}_i(k_x)\beta_{i+1}(k_x) \\ & + \sum_{i,k_x} t_{i,\perp} \beta^{\dagger}_i(k_x)\alpha_{i+1}(k_x) \Bigg) + \mathrm{h.c.} \\ & + \Bigg(V_{\mathrm{L},\alpha} \sum_{k,k_x} c^{\dagger}_{k,\mathrm{L}} \alpha_{\mathrm{L}}(k_x) + V_{\mathrm{L},\beta} \sum_{k,k_x} c^{\dagger}_{k,\mathrm{L}} \beta_{\mathrm{L}}(k_x) \Bigg) + \mathrm{h.c.} \\ & + \Bigg(V_{\mathrm{R},\alpha} \sum_{k,k_x} c^{\dagger}_{k,\mathrm{R}} \alpha_{\mathrm{R}}(k_x) + V_{\mathrm{R},\beta} \sum_{k,k_x} c^{\dagger}_{k,\mathrm{R}} \beta_{\mathrm{R}}(k_x) \Bigg) + \mathrm{h.c.}. \end{aligned} \tag{3}$$

The electrical transport in the coupled NGR proceeds as it does through two conduction channels, α and β, respectively. Owing to the orbit coupling between conducting graphene and insulating substrate where both channels have differences in essence, the new hybridized orbital energy levels for α and β are $E_{\alpha} = (e_m + e_p - \sqrt{(e_m - e_p)^2 + 4V^2})/2$ and $E_{\beta} = (e_m + e_p + \sqrt{(e_m - e_p)^2 + 4V^2})/2$, respectively; $t_{i,\alpha} = t_i(k_x)\sin^2\theta$ and $t_{i,\beta} = t_i(k_x)\cos^2\theta$ are effective hopping integrals in each individual channel; $t_{i,\perp} = t_i(k_x)\sin\theta\cos\theta$ is the crossing hopping integral between those channels; $V_{\mathrm{L(R)}\alpha} = V_{\mathrm{L(R)}}\sin\theta$ and $V_{\mathrm{L(R)}\beta} = V_{\mathrm{L(R)}}\cos\theta$ are coupling interactions between the α and β channels and the left (right) electrode. This two-channel model is depicted in figure 2. We assign index numbers to each of the α and β operators from 1 to $2N$ and redefine them as $A_i (i = 1\text{–}2N)$ for convenient calculation. The new representation of the Hamiltonian in A_i operator is $H = H_0 + H_I$, where

$$H_0 = \sum_{k,\mu\in \mathrm{L,R}} \epsilon_{k,\mu} c^{\dagger}_{k,\mu} c_{k,\mu} + \sum_{i=1,k_x}^{2N} E_i A^{\dagger}_i(k_x) A_i(k_x) \tag{4}$$

and

$$\begin{aligned} H_I = & \sum_{i=1,k_x}^{2N} (t_{i,\alpha}(k_x) A^{\dagger}_i(k_x) A_{i+1}(k_x)\Theta(N-1-i) \\ & + t_{i,\beta}(k_x) A^{\dagger}_i(k_x) A_{i+1}(k_x)\Theta(i-N-1)) + \mathrm{h.c.} \end{aligned}$$

$$+\sum_{i=1,k_x}^{2N} t_{i,\perp}(k_x)(A_i^\dagger(k_x)A_{i+N+1}(k_x) + A_{N+i}^\dagger(k_x)A_{i+1}(k_x))\Theta(N-1-i) + \text{h.c.} + V_{\mathrm{L},1}\sum_{k,k_x} c_{k,1}^\dagger A_1(k_x) + V_{\mathrm{R},N}\sum_{k,k_x} c_{k,N}^\dagger A_N(k_x) + \text{h.c.} + V_{\mathrm{L},N+1}\sum_{k,k_x} c_{k,N+1}^\dagger A_{N+1}(k_x) + V_{\mathrm{R},2N}\sum_{k,k_x} c_{k,2N}^\dagger A_{2N}(k_x) + \text{h.c.}, \quad (5)$$

with coupling interactions $V_{\mathrm{L},1} = V_{\mathrm{L},\alpha}$, $V_{\mathrm{R},N} = V_{\mathrm{R},\alpha}$, $V_{\mathrm{L},N+1} = V_{\mathrm{L},\beta}$ and $V_{\mathrm{R},2N} = V_{\mathrm{R},\beta}$ and Θ is the step function. The current formula of equation (2) requires that we include the calculation for the retarded Green's function, $G^{\mathrm{r}}_{i,j}(k_x,t) = \langle\langle A_i(k_x); A_j^\dagger(k_x)\rangle\rangle = -i\Theta(t)\{[A_i(k_x), A_j^\dagger(k_x)]\}$, which constructs the relation with self-energy, Σ^{r}, and bare Green's function, G_0^{r}, by $G^{\mathrm{r}} = G_0^{\mathrm{r}} + G_0^{\mathrm{r}}\Sigma^{\mathrm{r}}G^{\mathrm{r}}$. After employing the equation of motion for the Green's function, this leads to the equation

$$\langle\langle [A_i, H_I]; A_j^\dagger\rangle\rangle(k_x,E) = \sum_{p=1}^{2N}\Sigma^{\mathrm{r}}_{ip}(k_x,E)G^{\mathrm{r}}_{pj}(k_x,E), \quad (6)$$

from which the self-energy, $\sum^{\mathrm{r}}$, has $2N \times 2N$ dimensions, represented by

$$\Sigma^{\mathrm{r}} = \begin{pmatrix} D_{\mathrm{L}} - i\frac{\Gamma_{\mathrm{L}}^1}{2} & t_{1,\alpha} & & & & \vdots \\ t_{1,\alpha}^* & 0 & t_{2,\alpha} & & & \vdots \\ & t_{1,\alpha}^* & \ddots & \ddots & & \vdots \\ & & \ddots & 0 & t_{1,\alpha} & \vdots \\ & & & t_{1,\alpha}^* & D_{\mathrm{R}} - \mathrm{i}\frac{\Gamma_{\mathrm{R}}^N}{2} & \vdots \\ \cdots & \cdots & \cdots & \cdots & \cdots & \cdots \\ & t_{1,\perp}^* & & & & \vdots \\ t_{1,\perp}^* & & t_{2,\perp}^* & & & \vdots \\ & t_{2,\perp}^* & & t_{1,\perp}^* & & \vdots \\ & & \ddots & & \ddots & \vdots \\ & & & & & \vdots \end{pmatrix} \begin{pmatrix} t_{1,\perp} & & & & \\ & t_{2,\perp} & & & \\ t_{2,\perp} & & t_{1,\perp} & & \\ & \ddots & & \ddots & \\ \cdots & \cdots & \cdots & \cdots & \cdots \\ D_{\mathrm{L}} - i\frac{\Gamma_{\mathrm{L}}^{N+1}}{2} & t_{1,\beta} & & & \\ t_{1,\beta}^* & 0 & t_{2,\beta} & & \\ & t_{2,\beta}^* & \ddots & \ddots & \\ & & \ddots & 0 & t_{1,\beta} \\ & & & t_{1,\beta}^* & D_{\mathrm{R}} - i\frac{\Gamma_{\mathrm{R}}^{2N}}{2} \end{pmatrix}_{2N\times 2N}, \quad (7)$$

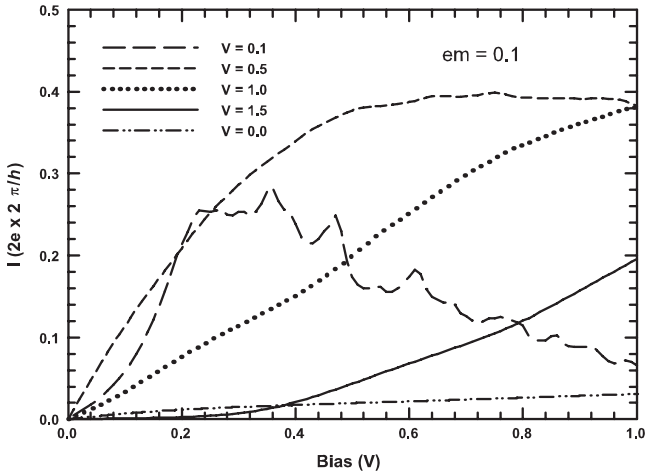

Figure 3. The current-bias profiles for various couplings V, under the assumption that the energy level of the substrate is constant.

where $t_{1(2),\alpha}$, $t_{1(2),\beta}$ and $t_{1(2),\perp}$ are the hopping integrals in both individual channels and their crossing as $i = 1, 3, \ldots$ ($i = 2, 4, \ldots$); the spectral functions $\Gamma_\alpha^j = i2\pi\sum_{k,\alpha} V_{\alpha,j}^* V_{\alpha,j}\delta(\epsilon - \epsilon_{k,\alpha})$ ($j = 1, N, N+1, 2N$; $\alpha = \mathrm{R}, \mathrm{L}$), corresponding to the density of states (DOS) of electrodes. In the wide band limit for metallic electrodes, the spectral functions can be approximated to a constant, and $D \approx -\frac{\Gamma}{\pi}\ln|\frac{W/2+E}{W/2-E}|$, where W is the bandwidth of the electrode [18].

The number of honeycomb unit cells in the width of our sample, $n_\square$, is 5 and the energy parameters of the Hamiltonian equation (1) used in our calculations in units of eV are $e_p = 0$, $V_{\mathrm{L(R)}} = 1.0$, $t = 2.598$, and the DOS in the spectral function, $\sum_{k,\alpha=\mathrm{L,R}}\delta(\epsilon - \epsilon_{k,\alpha})$, is approximated as the inverse of the electrode's bandwidth, $\frac{1}{W}$, where $W = 30$. The total current $I = I_\alpha + I_\beta$ is calculated by means of employing the above energy variables for both channels in equation (2).

3. Results and discussion

In our model, two energy parameters, e_m and V, are used to simulate the intrinsic property of a substrate coupling to the NGR, where e_m is the orbital energy level of the substrate and V is the orbital hybridization interaction between the substrate and NGR. If the carrier transfer between the NGR and substrate is not conducted by means of tunneling, two orbits should be overlapping within the bandwidth of the NGR. Unequivocally, if e_m is closer to e_p, the two orbits will hybridize effectively to each other and the transport along the NGR will be influenced apparently. This conduction variation by different couplings is shown in figure 3 with constant e_m, which is slightly higher than e_p; as the figure shows, at small V ($V = 0.5$) the current increases significantly compared with a non-coupling NGR ($V = 0$), which implies a carrier contribution from the substrate surface, i.e. surface charges [15], to the NGR via coupling. In contrast to the small coupling, at large V ($V = 1.0$–1.5) a conducting–insulating transition occurs, which implies a large hybridization will localize the transport carriers in the NGR. The experimental results show that the

bandgaps open as the few-layer-thick graphite is deposited on the substrates and the gap width increases as the thickness of the graphite decreases. In addition, the mechanism of bandgap opening is proposed, owing to the Dirac point rehybridization induced by the substrate coupling [15]. Obviously, this mechanism is consistent with our results, related to the bandgap increase corresponding to our conducting–insulating transition via the coupling increase. Although a bandgap has been confirmed to exist in the NGR [19, 20], however, the coupling self-energy between the NGR and the electrodes in equation (7) and the thermal effect at room temperature will suppress the intrinsic or extrinsic gap of the graphene induced from size scale [19, 20] or substrate coupling, respectively [15]. Therefore, the current is continuous from zero bias in figure 3. These intrinsic or extrinsic gaps will become distinct as the thermal excitation is suppressed with the temperature decreasing. In contrast, as the temperature is higher than room temperature, the substrate coupling effect will be reduced.

In particular, at very small V ($V = 0.1$), a negative resistance is present at a relatively large bias. Because we employ the constant DOS approximation to the metallic electrode, our theory does not support the possibility of the negative resistance coming from the coupling with the electrodes. This constant DOS approximation is suitable for wide band metal, where the band dispersion near the Fermi energy is linear approximately. Regarding non-constant DOS cases, the metallic electrode with finite bandwidth in the one-dimensional approximation of the spectral function becomes energy-dependent and has the exact solution, $\Gamma^j_\alpha(\epsilon) = \frac{V^*_{\alpha,j}V_{\alpha,j}}{\frac{\epsilon-E_{\mathrm{L(R)}}}{2}+i\sqrt{(\frac{W}{4})^2-(\frac{\epsilon-E_{\mathrm{L(R)}}}{2})^2}}$, where $E_{\mathrm{L(R)}}$ is the eigenvalue of the left (right) end heads of the electrode, which will be shifted by the applied bias. In this finite bandwidth approximation, our private calculation reveals that the negative differential conductance (NDR) occurs under proper interactions and applied bias. Through the investigation of the band structure of the coupled NGR, the negative resistance comes from the current redistribution between I_α and I_β through bias. Because of the new orbital energy levels, E_α and E_β, where E_α is lower than E_β, the current attributions from both channels are not equivalent and the α channel is dominant in conduction, which can be verified by turning off V, and making the E_α approach the energy level of the NGR, e_p. Due to the Fermi level being shifted by the bias application, the relative weight of conduction from each channel will vary. If these E_α and E_β are not widely separated (at very small V), the Fermi level crosses the relatively high-conductive α bands predominantly at small bias leading to a normal conduction, namely, the current increases as the bias increases. In contrast, at large bias, the predominant band crossing by Fermi level changes to the less-conductive β channels, consequently resulting in negative resistance.

In the presence of a magnetic field perpendicular to the plane of the NGR, $B = (0, 0, B)$, the hopping element of the Hamiltonian in the tight-binding model needs to be modified with Peierl's phase shift [21–23] if the hopping path has a component which sweeps the magnetic field perpendicularly.

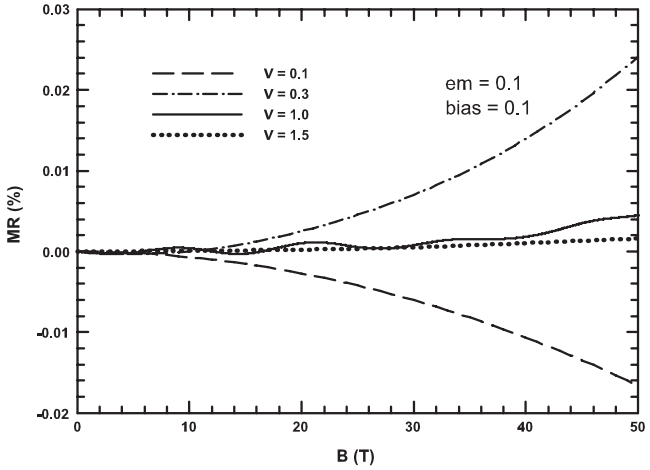

Figure 4. The magnetoresistance is negative at small coupling V and positive at large V. The unit of magnetic field is tesla.

The Hamiltonian then becomes

$$H = \sum_{i,j} t_{i,j} e^{i(k\cdot(r_i-r_j)+\frac{2\pi}{\Phi_0}\int_i^j A(r)\cdot dr)} = \sum_{i,j} t'_{i,j} e^{ik\cdot(r_i-r_j)}, \quad (8)$$

where $t_{i,j}$ is the hopping integral and Φ_0 is the unit magnetic flux. We can choose the position-dependent Landau gauge $A(r)$ as $A(r) = (-By, 0, 0)$. Obviously, this position-dependent phase shift will influence the transport property. We need to modify the Peierl phase shift to hopping integrals, $t_{1,\alpha}$, $t_{1,\beta}$ and $t_{1,\perp}$, only because those hopping paths can couple with the magnetic flux. Thus, the magnetic flux integral is $\Phi_{i,j} = \int_i^j A(r)\cdot dr$, which passes through the area, $\Delta_{i,j} = (y_i - y_j)a/2$, where y_n is the distance from the n point to the right end point and a is the honeycomb lattice constant. Based on the definition of magnetoresistance (MR), $\mathrm{MR} = (R(B) - R(0))/R(0)$, which is equal to $\Delta I/I(B)$, where $R(B)$ and $I(B)$ are the resistance and the current at an applied magnetic field, respectively. The theoretical results reveal the positive or negative MR corresponds to various V and the MR turns from negative to positive with the increase of V, as shown in figure 4. The interaction V of orbital hybridization in our model actually implies the strength of localization to carriers. We propose the negative MR, revealing small V in our model is consistent with the physics which has predicted that the negative MR of the NGR is attributed to weak localization (WL) [24, 25], where the suppression and creation of weak localization in graphene has been studied in some proposals [26–28]. The increase of V means changing from weak localization to strong localization and eventually to positive MR. It is rational to realize in our model that the weak substrate coupling ($V = 0.1$ in our case) is equivalent to atomically sharp scatterers for graphene [27] as a potential perturbation, where the effective scattering potential is not smooth because the current-bias behavior, as shown in figure 3, is different from other V, and it provides the backward scattering to construct WL; consequently, the applied magnetic field will destroy the quantum interferences in moving trajectories with

resulting negative MR. In contrast, as V increases, the substrate coupling will be outside WL because the effective scattering potential is smooth and the backward scattering is diminished with resulting positive MR. In addition, the MR represents almost no variation at large V, because the carrier localization is significant at very strong orbital hybridization; an even stronger magnetic field will not change the MR significantly.

To conclude, we propose a model that simulates the electrical conduction of a substrate-coupled nanographene ribbon. The coupling between the substrate and the nanographene ribbon increases the conduction of the nanographene ribbon when compared with a non-substrate-coupled nanographene ribbon, especially at small coupling; eventually, the large coupling suppresses the conduction. The magnetoresistance of the nanographene is negative at small coupling and turns out to be positive as the coupling increases.

Acknowledgments

This work was supported by the National Science Council in Taiwan through grant nos. NSC-95-2112-M-390-002-MY3 and 96-2120-M-006-001. The hospitality of the National Center for Theoretical Sciences, Taiwan, where the work was initiated, is gratefully acknowledged.

References

[1] Heinze S, Tersoff J, Martel R, Derycke V, Appenzeller J and Avouris Ph 2002 *Phys. Rev. Lett.* **89** 106801
[2] Appenzeller J, Knoch J, Radosavljevic M and Avouris Ph 2004 *Phys. Rev. Lett.* **92** 226802
[3] Bachtold A, Hadley P, Nakanishi T and Dekker C 2001 *Science* **294** 1317
[4] Saito R, Dresselhaus G and Dresselhaus M S 1998 *Physical Properties of Carbon Nanotubes* (London: Imperial College Press)
[5] Geim A K and Novoselov K S 2007 *Nat. Mater.* **6** 183
[6] Novoselov K S, Geim A K, Morozov S V, Jiang D, Zhang Y, Dubonos S V, Gregorieva I V and Firsov A A 2004 *Science* **306** 666
[7] Meyer J C, Geim A K, Katsnelson M I, Novoselov K S, Booth T J and Roth S 2007 *Nature* **446** 60
[8] Morozov S V, Novoselov K S, Katsnelson M I, Schedin F, Elias D C, Jaszczak J A and Geim A K 2008 *Phys. Rev. Lett.* **100** 016602
[9] Novoselov K S, Geim A K, Morozov S V, Jiang D, Katsnelson M I, Grigorieva I V, Dubonos S V and Firsov A A 2005 *Nature* **438** 197
[10] Ohta T, Bostwick A, Seyller T, Horn K and Rotenberg E 2006 *Science* **313** 951
[11] Nillsson J, Castro Neto A H, Guinea F and Peres N M R 2007 *Phys. Rev.* B **76** 165416
[12] Xu Z, Zheng Q-S and Chen G 2007 *Appl. Phys. Lett.* **90** 223115
[13] Yoon Y and Guo J 2007 *Appl. Phys. Lett.* **91** 073103
[14] Mermin N D 1968 *Phys. Rev.* **176** 250
[15] Zhou S Y, Gweon G-H, Fedorov A V, First P N, Heer W A D, LEE D-H, Guinea F, Neto A H C and Lanzara A 2007 *Nat. Mater.* **6** 770
[16] Calizo I, Bao W, Miao F, Lau C N and Balandin A A 2007 *Appl. Phys. Lett.* **91** 201904
[17] Haug H and Jauho A-P 1998 *Quantum Kinetics in Transport and Optics of Semiconductors* (Berlin: Springer)
[18] Bruus H and Flensberg K 2004 *Many-Body Quantum Theory in Condensed Matter Physics* (Oxford: Oxford University press) chapter 9
[19] Son Y-W, Cohen M L and Louie S G 2006 *Phys. Rev. Lett.* **97** 216803
[20] Han M Y, Ozyilmaz B, Zhang Y and Kim P 2007 *Phys. Rev. Lett.* **98** 206805
[21] Wakabayashi K, Fujita M, Ajiki H and Sigrist M 1999 *Phys. Rev.* B **59** 8271
[22] Chang C P, Lu C L, Shyu F L, Chen R B, Huang Y C and Lin M F 2005 *Physica* E **27** 82
[23] Chang C P, Lu C L, Shyu F L, Chen R B, Fang Y K and Lin M F 2004 *Carbon* **42** 2975
[24] Kechedzhi K, McCann E, Fal'ko V I, Suzuura H, Ando T and Altshuler B L 2007 *Eur. Phys. J.* **148** 39 special topics
[25] Gorbachev R V, Tikhonenko F V, Mayorov A S, Horsell D W and Savchenko A K 2007 *Phys. Rev. Lett.* **98** 176805
[26] Morozov S V, Novoselov K S, Katsnelson M I, Schedin F, Ponomarenko L A, Jiang D and Geim A K 2006 *Phys. Rev. Lett.* **97** 016801
[27] McCann E, Kechedzhi K, Fal'ko V I, Suzuura H, Ando T and Altshuler B L 2006 *Phys. Rev. Lett.* **97** 146805
[28] Khveshchenko D V 2006 *Phys. Rev. Lett.* **97** 036802